Proceedings of the 21st ICSMGE, Vienna, Austria, 14 – 19 June 2026. Pistrol, Adam & Schweiger (eds.)
Published by: ÖGG, Austrian Society for Geomechanics, Salzburg, Austria, ISBN 978-3-9503898-4-5
https://doi.org/10.53243/ICSMGE2026-640

Feasibility of conditional VAE-based generative design for slope nail reinforcement

Taegu Kim, Hyunsoo Kim, Tae Sup Yun
School of Civil and Environmental Engineering, Yonsei University, Seoul, South Korea, taesup@yonsei.ac.kr

Younjong Sim
Land and Housing Research Institute, LH, Daejeon, South Korea

ABSTRACT: Generative artificial intelligence (AI) is emerging as a powerful tool for automating engineering design. Conditional Variational Autoencoders (CVAEs) are effective for parametric design problems, enabling controllable generation using specific design requirements as conditions while maintaining diversity via latent sampling. This study applies a CVAE framework to slope nail reinforcement design, a problem balancing variables like geotechnical properties, safety targets, cost, and constructability. In this framework, the CVAE takes two-layer geotechnical properties and a target factor of safety (FS) as input to generate candidate layouts defined by nail number, length, spacing, inclination, and insertion position. A learned FS surrogate rapidly evaluates candidates, efficiently filtering noncompliant designs while preserving diverse, feasible alternatives. Trained on LEM simulation data and tested on two stratigraphies, the framework yields multiple layouts meeting the target FS. For slopes with a weaker lower layer, the CVAE accurately generates on-target designs and the surrogate's predictions are reliable. Conversely, for slopes with a weaker upper layer (causing complex failure modes), accuracy declines, yet the framework still identifies feasible, near-target solutions. Results demonstrate that conditional generative design offers controllability, diversity, and fast verification, supporting faster, informed decision-making in early-stage geotechnical reinforcement design.

KEYWORDS: Generative design, conditional variational autoencoder, slope stability, soil nailing, surrogate model.

1 INTRODUCTION

Generative artificial intelligence (AI) offers a promising new approach to automating complex engineering design tasks (Regenwetter, Nobari and Ahmed, 2022; Liao et al., 2024). By leveraging deep learning architectures, generative models such as variational autoencoders (VAEs) and generative adversarial networks (GANs) learn from large datasets to capture latent structural patterns and generate diverse solutions tailored to design requirements (Kingma and Welling, 2013). In particular, VAEs provide advantages for parametric design through their continuous latent spaces, and conditional VAEs (CVAEs) extend this capability by incorporating external design conditions, enabling targeted and controllable generation (Sohn, Yan and Lee, 2015). Prior studies have applied CVAE-based approaches to the design of space truss structures, wall layouts, and pedestrian bridges, demonstrating flexibility and effectiveness in handling complex constraints (Danhaive and Mueller, 2021; Bucher et al., 2023; Balmer et al., 2024).

This study applies a CVAE framework to slope nail reinforcement design. While widely used, determining an optimal layout remains a complex and iterative process. Engineers must consider multiple interacting parameters (number, length, spacing, inclination, and insertion position), which all influence stability factors of safety (FS). Although metaheuristic techniques such as genetic algorithms and particle swarm optimization have been explored for slope nail design, they have generally been applied to simplified, single-layer slope conditions (Patra and Basudhar, 2005; Fan and Luo, 2008; Shirgir et al., 2023). They also yield single solutions and require substantial computation, limiting their practicality in exploratory early design stages.

To address these challenges, we propose a CVAE-based generative framework that automatically produces multiple slope nail reinforcement layouts conditioned on given slope conditions and a target FS. The input to the model includes a two-layer slope condition, defined by geotechnical properties and layer thicknesses, along with the target FS. The output consists of five reinforcement design parameters: the number, length, spacing, inclination, and insertion position of nails. For simplicity, slope geometry and nail material properties are fixed in this study.

To train the model, a dataset of 6,000 samples was constructed using Hyrcan, a limit equilibrium method (LEM) software with Python integration for automated simulation. Each sample comprises a unique combination of slope condition, reinforcement layout, and the resulting FS value, sampled across a range near the target FS to ensure structural validity and design diversity.

While the CVAE enables flexible design generation through probabilistic sampling in the latent space, it does not guarantee precise performance targets. To overcome this limitation, we incorporate a neural network-based surrogate model to estimate the FS of generated layouts and automatically filter those failing to meet safety criteria. This filtering step ensures only feasible configurations are retained.

Ultimately, the proposed framework offers engineers multiple feasible reinforcement layouts for a given slope condition and target FS. These alternatives enable flexible decision-making based on cost, constructability, and site-specific constraints. To validate the framework, we apply it to two representative slope conditions with distinct subsurface profiles and assess the generated layouts.

2 PROBLEM SETUP AND DATA CONSTRUCTION

Slope nail reinforcement enhances slope stability by mobilizing resistance along potential slip surfaces. The design process involves selecting appropriate reinforcement variables based on given ground conditions, while satisfying internal and external stability requirements. This section introduces the problem setup, the stability criteria for feasible designs, and the construction of the simulation-based dataset for model training.

2.1 *Design variables*

Figure 1 illustrates the input and output variables for the generative design framework. The input variables, shown in black, define the geotechnical conditions of the two-layer slope, its geometry, and the target safety requirement. The output variables, shown in blue, define the resulting nail reinforcement

layout. These parameters form the parametric basis of the model.

The model's input consists of eight variables: the geotechnical properties (cohesion, friction angle, unit weight) and thickness for both the upper layer (c_1, ϕ_1, γ_1, H_1) and the lower layer (c_2, ϕ_2, γ_2, H_2). In addition, the target factor of safety (FS_{req}) is provided as a conditioning input.

The model's output is a vector of five design variables that define the reinforcement layout: the number of nails (n), nail length (L), spacing (s), insertion angle (α), and starting offset from the slope crest (x).

For this study, the overall slope geometry is fixed, with a total height of 15 m and a slope angle (β) of 63.4° (equivalent to a 2:1 slope). While fixed here, these could be treated as variable inputs in future work.

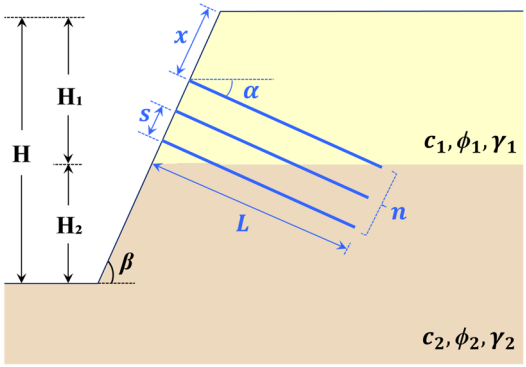

Figure 1. Schematic of input and output variables for the generative design framework.

2.2 *Stability criteria*

To ensure structural validity, both external and internal stability must be satisfied according to engineering standards (Lazarte et al., 2015).

External stability is evaluated by computing the global factor of safety (FS) through limit equilibrium analysis (Duncan, 1996). Design codes generally require a minimum FS of 1.5 under static, dry conditions.

Internal stability concerns the capacity of each nail to resist axial loading from slope movement, limited by allowable tensile and bond capacities. These allowable capacities are determined by applying safety factors to the theoretical strengths of the nail components. The allowable tensile and bond resistances are given by:

$$T_{tensile,allow} = \frac{1}{1.5} \cdot \frac{\pi}{4} D_{bar}{}^2 f_y \quad (1)$$

$$T_{bond,allow} = \frac{1}{2} \cdot \tau_b \, \pi \, D_{grout} \, L \quad (2)$$

where key reinforcement properties are kept constant to simplify the problem setup: the steel bar diameter (D_{bar}) and yield strength (f_y) are fixed at 32 mm and 415 MPa, respectively, and the grout diameter (D_{grout}) is 100 mm. The bond strength between the grout and soil, τ_b, is set based on soil type, with values of 300, 150, 80, and 60 kN/m for soft rock, weathered rock, weathered soil, and sand, respectively.

The allowable axial capacity is defined as the lesser of the two values, reflecting the most critical failure mechanism. This capacity is precomputed and applied in the LEM analysis as the working load of each nail. This approach ensures internal stability is satisfied, making the external FS the sole governing performance criterion for the generative model.

2.3 *Dataset construction*

A simulation-based dataset was developed to train the CVAE model, comprising diverse slope conditions and corresponding reinforcement designs. The data generation process involved two main steps as illustrated in Figure 2: (1) sampling slope conditions and (2) sampling reinforcement designs for each slope. All simulations were performed using Hyrcan, a LEM-based software with Python integration for automated analysis (Mikola, 2023).

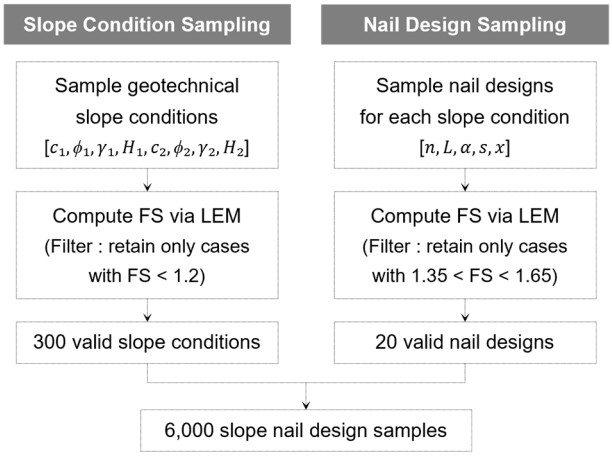

Figure 2. Dataset construction process: slope condition and nail design sampling.

In the first step, 300 valid two-layer slope conditions were generated by randomly sampling geometric and geotechnical parameters. The total slope height was fixed at 15 m, and the thicknesses of the upper and lower layers were independently sampled with a minimum of 3 m. A soil type was randomly selected for each layer from four representative categories, e.g., soft rock, weathered rock, weathered soil, and sand. Geotechnical properties were then sampled within the ranges specified in Table 1. After computing the FS using LEM analysis, only slope conditions with an unreinforced FS below 1.2 were retained. This procedure was repeated until 300 valid slope conditions were obtained.

Table 1. Sampling ranges of soil properties.

Soil Type	γ (kN/m³)	c (kPa)	ϕ (°)
Sand (SD)	16–19	0–5	30–38
Weathered Soil (WS)	17-19	5-25	22-30
Weathered Rock (WR)	20-22	30-80	30-38
Soft Rock (SR)	22-24	80-150	35-42

In the second step, reinforcement designs were generated for each slope condition by randomly sampling five design variables as specified in Table 2. Sampling was repeated until 20 reinforcement layouts per slope were found that satisfied an FS range of 1.35 to 1.65. This range was selected to ensure both structural adequacy and design diversity.

Table 2. Sampling ranges of nail design variables.

Design Variable	Symbol	Range	Unit
Number of nails	n	3–10	-
Nail length	L	6–18	m
Nail inclination	α	10–30	°
Nail spacing	s	1.0–2.5	m
Nail start offset	x	0–10	m

As a result, the dataset contained 6,000 valid samples. Each sample comprised a slope condition vector (C_i), a reinforcement design vector (Y_i), and the corresponding FS value (FS_i) calculated through LEM analysis.

3 CVAE-BASED GENERATIVE DESIGN WORKFLOW

This section outlines the integrated workflow used for conditional generative design of slope nail reinforcement, as illustrated in Figure 3. The framework consists of three sequential stages: (1) CVAE training, (2) design generation, and (3) design filtering using a pre-trained surrogate model.

(a)

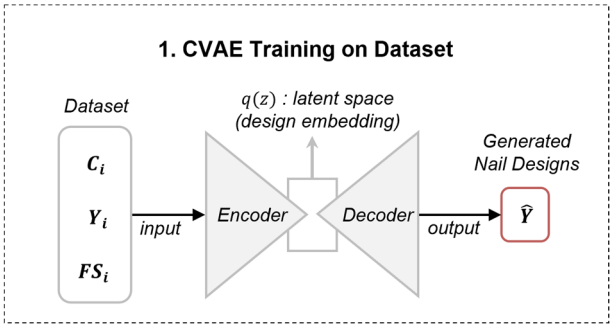

(b)

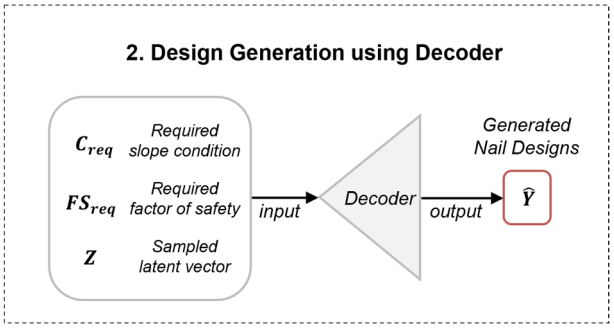

(c)

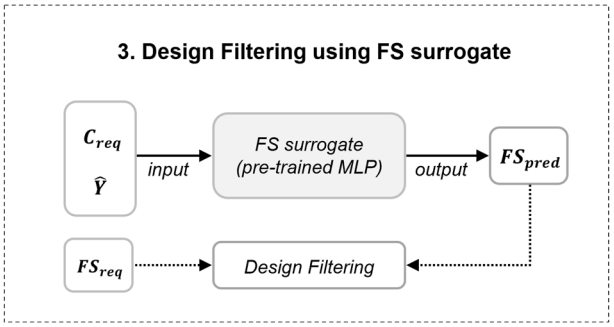

Figure 3. The proposed CVAE-based generative design workflow: (a) CVAE training, (b) design generation, and (c) design filtering.

3.1 *CVAE training on dataset*

In the first stage of the workflow (Figure 3a), the CVAE is trained on the simulation dataset from Section 2.3. The model learns to generate reinforcement layouts that satisfy given slope conditions and safety requirements by capturing their underlying relationships in a compact latent representation.

For each training sample, the encoder receives the slope condition (C_i), reinforcement layout (Y_i), and factor of safety (FS_i) as inputs. These are encoded into a latent distribution, $q(z)$, which represents how reinforcement layouts vary with different conditions. During training, $q(z)$ is regularized to approximate a standard Gaussian distribution, $\mathcal{N}(0, I)$, to ensure stable sampling during the generation. A latent vector, Z, sampled from $q(z)$ is then passed to the decoder. The decoder reconstructs the layout, $\hat{Y}$, while being conditioned on the same C_i and FS_i. Through this process, the decoder learns to generate valid designs from given conditions and latent variables.

The encoder and decoder are each composed of two-layer fully connected networks with 512 hidden units, batch normalization, and ReLU activations. The latent space dimension is set to 64. The model handles mixed data types: the number of nails is represented as an 8-dimensional one-hot vector, while the remaining four continuous variables are normalized to [0,1].

The training loss is composed of three terms: categorical cross-entropy, negative log-likelihood, and Kullback–Leibler divergence. Several techniques are applied to improve convergence, including KL warm-up, free-bits regularization, and Gumbel-softmax for differentiable sampling. Training was conducted for 300 epochs using the Adam optimizer with a learning rate of 1e-4 and a batch size of 256. The KL warm-up was set to 50 epochs, and the Gumbel-softmax temperature was 0.5.

To improve sensitivity to the design conditions, a y-skip architecture is employed, injecting the conditioning vector (C_i, FS_i) into every layer of both the encoder and decoder (Bucher et al., 2023). This enhances stability and the model's ability to reflect condition-dependent variations.

3.2 *Design generation using decoder*

In the second stage of the workflow (Figure 3b), the trained decoder is used to generate reinforcement layouts. It takes three inputs: a required slope condition (C_{req}), a target factor of safety (FS_{req}), and a latent vector (Z) sampled from the standard normal distribution, $\mathcal{N}(0, I)$.

Since the decoder has learned to reconstruct valid layouts from latent vectors and design conditions during training, it can produce diverse layouts by sampling multiple latent vectors for the same (C_{req}, FS_{req}) pair. This approach enables the generation of multiple feasible reinforcement layouts from a single design requirement.

Because the CVAE is a probabilistic generative model, it is not guaranteed that all generated layouts will exactly meet FS_{req}. Deviations arise from randomness in latent sampling. Therefore, a subsequent filtering step is applied to retain only those layouts whose predicted FS is sufficiently close to the target value.

3.3 *Design filtering using FS surrogate*

In the final stage of the workflow (Figure 3c), a pre-trained neural surrogate model evaluates the safety performance of generated layouts and filters them without repeating LEM simulations. The surrogate, implemented as a multilayer perceptron (MLP), takes the concatenated vector of the slope condition (C_{req}) and a generated layout ($\hat{Y}$) as input and outputs a predicted factor of safety (FS_{pred}). Designs with FS_{pred} values sufficiently close to the target FS_{req} are retained as final candidates.

The surrogate was trained on a broader dataset of 48,000 samples from 1,200 slope configurations, which was generated following the same procedure described in Section 2.3. The dataset covers both safe and unsafe layouts to ensure robustness. Test results showed that the trained surrogate achieved a mean

absolute error below 0.03, indicating reliable filtering performance.

By decoupling the probabilistic generation from the surrogate-based verification, the framework maintains the diversity enabled by the CVAE while efficiently screening for candidates that meet engineering safety requirements. This balance provides a robust foundation for automated slope reinforcement design.

4 RESULTS

This section presents the generative design results for two representative slope configurations with distinct subsurface profiles. In both cases, the target factor of safety was set to FS_{req}=1.5. For each case, 300 reinforcement layouts were generated, evaluated via the limit equilibrium method (LEM) to obtain their true factor of safety (FS_{LEM}), and then filtered using the surrogate's prediction (FS_{pred}).

4.1 *Case 1: Stiff-Over-Weak Stratigraphy (WR–WS)*

Case 1 corresponds to an upper layer of weathered rock (WR) over a lower layer of weathered soil (WS), serving as a representative example of a stiff-over-weak stratigraphy. The slope consists of an upper layer (H_1=10.0 m, γ_1=21.0 kN/m^3, c_1=55.0 kPa, ϕ_1=34.0°) and a lower layer (H_2=5.0 m, γ_2=18.0 kN/m^3, c_2=15.0 kPa, ϕ_2=26.0°). The unreinforced slope had an FS_{LEM}=1.10.

Figure 4 displays the distribution of FS_{LEM} for the 300 generated layouts. The histogram peaks near the target value of FS_{req}=1.5, indicating that the CVAE tends to produce designs aligned with the requirement. However, the range of generated FS values is wide, extending from approximately 1.1 to 2.1, so not all designs are directly applicable.

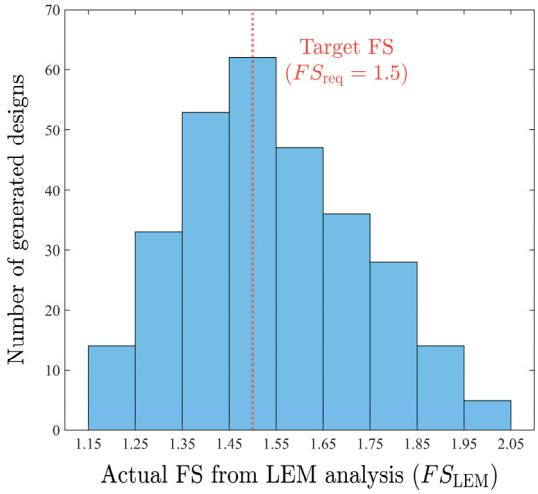

Figure 4. Distribution of FS_{LEM} for generated designs for Case 1 (WR-WS).

Figure 5 compares the true FS_{LEM} with the predicted FS_{pred}, showing strong overall agreement with the scatter concentrated around the one-to-one line. The shaded band indicates the acceptance window $1.45 < FS_{pred} < 1.55$, a symmetric tolerance of 0.05 around the target. Applying this filter retained 57 of the 300 layouts, which are highlighted as red dots in the figure.

Table 3 summarizes four representative layouts selected from the filtered set, categorized by different practical criteria. These options span distinct strategies while keeping the FS_{LEM} close to 1.5, allowing engineers to choose based on site constraints, economy, and constructability.

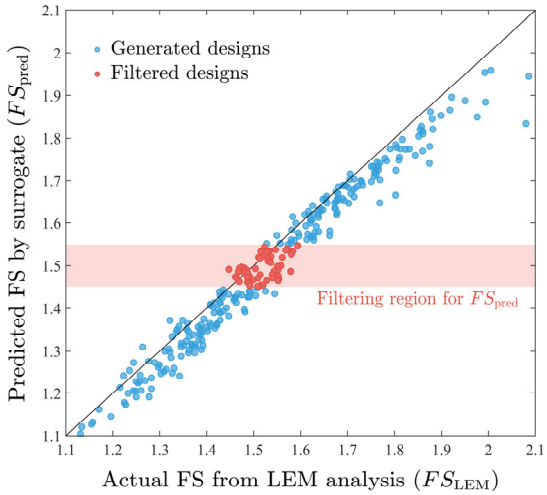

Figure 5. Surrogate-based filtering of generated designs for Case 1.

Table 3. Representative design alternatives for Case 1 (WR–WS).

Type	Min Cost (n×L)	Min Length (L)	Max Spacing (s)	Min offset (x)
n	3	6	4	5
L (m)	9.1	6.7	8.3	11.1
α (°)	14.0	30.0	16.7	23.5
s (m)	2.1	2.1	2.4	1.9
x (m)	10.0	4.2	6.6	1.1
Cost	27.2	40.4	33.3	55.5
FS_{pred}	1.47	1.47	1.45	1.49
FS_{LEM}	1.54	1.55	1.52	1.48

Figure 6 illustrates two example layouts from the filtered designs and their critical slip surfaces. Both an upper-focused pattern (left) and a lower-focused pattern (right) yield similar deep slip surfaces that pass through the weak lower layer. Notably, the lower-focused design (right) achieves a higher factor of safety with fewer nails, confirming that concentrating reinforcement in the lower portion provides a more economical solution when the lower layer governs stability.

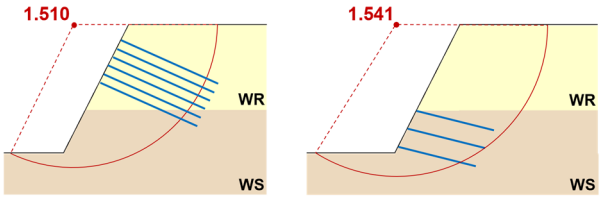

Figure 6. Representative reinforcement layouts and critical slip surfaces for Case 1 (WR-WS).

4.2 *Case 2: Weak-Over-Stiff Stratigraphy (WS–WR)*

Case 2 corresponds to a weak-over-stiff stratigraphy, a common condition found in practice, with an upper layer of weathered soil (WS) over a lower layer of weathered rock (WR). The slope consists of an upper layer (H_1=10.0 m, γ_1=18.0 kN/m^3, c_1=15.0 kPa, ϕ_1=26.0°) and a lower layer (H_2=5.0 m, γ_2=21.0 kN/m^3,

c_2=55.0 kPa, ϕ_2=34.0°). The unreinforced slope had an FS_{LEM} =0.99.

Figure 7 shows the distribution of FS_{LEM} for the 300 generated layouts. The distribution is bimodal, with a primary concentration near the target FS=1.5 and a second cluster appearing around FS=1.8. This indicates that for this stratigraphy, the CVAE frequently generates over-strengthened, non-target designs.

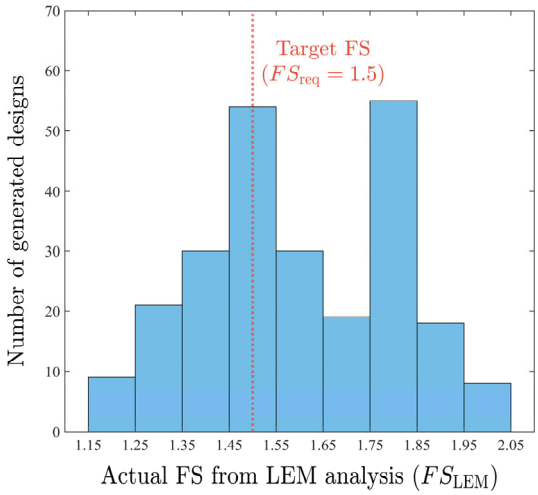

Figure 7. Distribution of FS_{LEM} for generated designs for Case 2 (WS-WR).

Figure 8 plots the true FS_{LEM} versus the predicted FS_{pred}. The shaded band in the figure indicates the acceptance window of $1.45 < FS_{pred} < 1.55$. Applying this window isolates a usable subset of designs, but the scatter about the one-to-one line is noticeably larger than in Case 1, particularly near the cluster regions around FS=1.50 and FS=1.82. Consequently, some designs with an actual FS_{LEM} close to the 1.5 target are incorrectly excluded, while a few inaccurate ones are admitted. In total, 45 of the 300 layouts were retained.

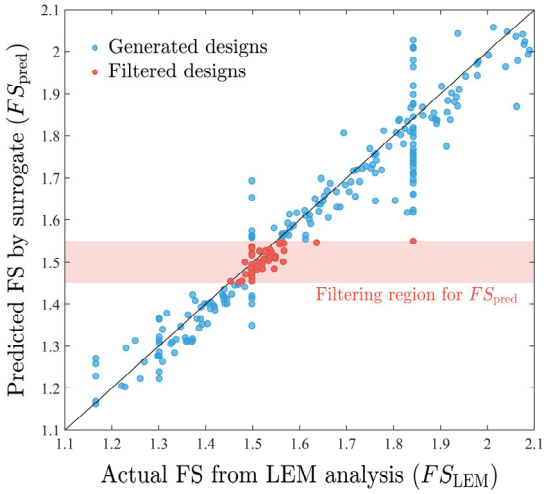

Figure 8. Surrogate-based filtering of generated designs for Case 2.

Table 4 summarizes representative layouts selected from the filtered set, categorized by the same practical criteria used in Case 1. These options remain sufficiently diverse and keep the FS_{LEM} near 1.5, confirming that the framework can deliver usable designs even under these more challenging conditions.

Table 4. Representative design alternatives for Case 2 (WS–WR).

Type	Min Cost (n×L)	Min Length (L)	Max Spacing (s)	Min offset (x)
n	3	6	3	4
L (m)	7.9	6.0	12.1	9.0
α (°)	16.7	23.2	23.8	24.1
s (m)	1.6	2.0	2.2	1.9
x (m)	3.5	0.0	5.7	0.0
Cost	23.6	36.0	36.3	35.9
FS_{pred}	1.45	1.55	1.49	1.51
FS_{LEM}	1.48	1.56	1.50	1.55

Figure 9 shows two representative layouts from the filtered designs. In Case 2, achieving a target FS can correspond to two distinct failure mechanisms: a shallow, upper-slope failure (left) or a deep, toe-controlled slip surface (right). The presence of two potential failure modes, and in particular the risk of the shallow, upper-slope failure becoming critical, is a key factor underlying the generation and prediction errors. When the upper layer is weak, minor changes in reinforcement can cause the critical slip surface to shift abruptly between these two modes, leading to sudden, discontinuous changes in the FS. Furthermore, once a shallow failure mode becomes critical, any changes to the deeper nails (e.g., their length or number) have little to no influence on the FS, further contributing to this discontinuity. This complex relationship is challenging for the CVAE and MLP models to learn, which explains both the generator's tendency to form an off-target cluster and the surrogate's reduced accuracy near the discontinuities.

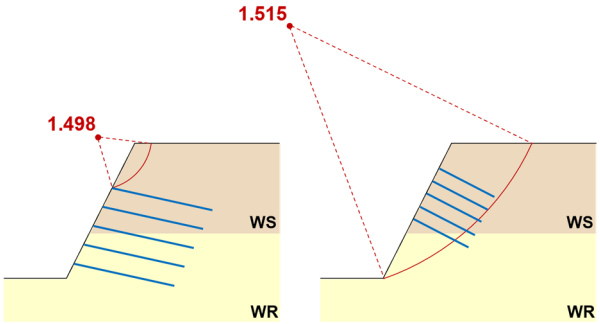

Figure 9. Two distinct failure mechanisms observed in Case 2 (WS-WR).

4.3 *Comparative discussion*

The two cases highlight how stratigraphy governs the model's effectiveness. In Case 1 (stiff-over-weak), the failure mode is stable, as the critical slip surface remains deep and the FS varies smoothly with reinforcement. This leads to reliable generation and accurate filtering. In Case 2 (weak-over-stiff), reinforcement can induce abrupt shifts between deep and shallow failure modes, creating a non-smooth mapping from design variables to FS. This results in decreased accuracy and an off-target generation cluster, a logical outcome given that both CVAE and MLP models are fundamentally optimized to learn smooth, continuous relationships from data. These observations suggest that the CVAE–surrogate framework is well-suited to slopes with predictable stability behavior but

remains serviceable, though less reliable, when complex, discontinuous failure mechanisms are present.

5 CONCLUSIONS

This study presented a conditional generative workflow that successfully automates the design of slope nail reinforcement. The proposed framework integrates a CVAE for generating a diverse range of design alternatives with a learned surrogate for rapid performance verification. Rather than producing a single deterministic optimum, this approach provides engineers with multiple, near-target, and design-diverse layouts, enabling a more informed balance between safety, economy, and constructability in the early stages of design. The case studies demonstrated the framework's effectiveness, particularly highlighting how its performance depends on whether the stratigraphy produces a smooth or discontinuous relationship between reinforcement and stability.

Despite its promising results, this study has limitations that suggest clear directions for future research. This work focused on feasibility under controlled conditions, such as fixed slope geometry and two-layer stratigraphies. Future work should extend the framework's applicability by expanding the conditioning set to include variable geometries, heterogeneous layering, groundwater effects, and seismic loading. Furthermore, the model and data strategies could be enhanced. The current random sampling of the dataset can under-represent critical regime-change regions, an issue that could be addressed by advanced data strategies like active sampling. The models themselves, CVAE and MLP, struggle with the discontinuous FS responses observed in complex cases. Therefore, exploring alternative architectures, such as ensemble surrogates or diffusion models known for better handling multimodal distributions, presents a promising avenue for improvement.

In conclusion, this study demonstrates the significant practical value of conditional generative design in geotechnical engineering. The framework offers controllability through target specifications, diversity through latent sampling, and rapid screening through learned verification. By providing a robust methodology for generating and evaluating multiple valid designs, this approach supports a faster, more flexible, and ultimately more effective geotechnical design process.

6 ACKNOWLEDGEMENTS

This work was supported by the National Research Foundation of Korea (NRF) grant funded by the Korean government (MSIT) (Nos. RS-2021-NR060085 and RS-2023-NR076991).

7 REFERENCES

Balmer, V., Kuhn, S.V., Bischof, R., Salamanca, L., Kaufmann, W., Perez-Cruz, F. and Kraus, M.A. 2024. Design space exploration and explanation via conditional variational autoencoders in meta-model-based conceptual design of pedestrian bridges. *Automation in Construction*, 163, 105411.

Bucher, M.J.J., Kraus, M.A., Rust, R. and Tang, S. 2023. Performance-based generative design for parametric modeling of engineering structures using deep conditional generative models. *Automation in Construction,* 156, 105128.

Danhaive, R. and Mueller, C.T. 2021. Design subspace learning: structural design space exploration using performance-conditioned generative modeling. *Automation in Construction*, 127, 103664.

Duncan, J.M. 1996. State of the art: limit equilibrium and finite-element analysis of slopes. *Journal of Geotechnical Engineering,* 122(7), 577–596.

Fan, C.C. and Luo, J.H. 2008. Numerical study on the optimum layout of soil-nailed slopes. *Computers and Geotechnics*, 35(4), 585–599.

Kingma, D. P. and Welling, M. 2013. Auto-encoding variational bayes. *arXiv:1312.6114*.

Lazarte, C. A., et al. 2015. *Geotechnical Engineering Circular No. 7: Soil Nail Walls—Reference Manual (Report No. FHWA-NHI-14-007)*. Washington, DC: National Highway Institute (US).

Liao, W., Lu, X., Fei, Y., Gu, Y. and Huang, Y. 2024. Generative AI design for building structures. *Automation in Construction*, 157, 105187.

Mikola, R.G. 2023. HYRCAN: a comprehensive limit equilibrium software package for 2D slope stability analysis. *Authorea Preprints.*

Patra, C.R. and Basudhar, P.K. 2005. Optimum design of nailed soil slopes. *Geotechnical and Geological Engineering*, 23(3), 273–296.

Regenwetter, L., Nobari, A.H. and Ahmed, F. 2022. Deep generative models in engineering design: a review. *Journal of Mechanical Design*, 144(7), 071704.

Shirgir, S., Shamsaddinlou, A., Zare, R.N., Zehtabiyan, S. and Bonab, M.H. 2023. An efficient double-loop reliability-based optimization with metaheuristic algorithms to design soil nail walls under uncertain condition. *Reliability Engineering and System Safety*, 232, 109077.

Sohn, K., Yan, X. and Lee, H. 2015. Learning structured output representation using deep conditional generative models. *Advances in Neural Information Processing Systems*, 28, 3483–3491.